Appendix

A Dual Role for the Chromatin Reader ORCA/LRWD1 in Targeting the Origin Recognition Complex to Chromatin

Sumon Sahu[1]*, Babatunde E. Ekundayo[1,2,]*, Ashish Kumar[1], and Franziska Bleichert[1#]

[1]Department of Molecular Biophysics and Biochemistry, Yale University, New Haven, CT, USA
[2]Current affiliation: Laboratory of Biological Electron Microscopy, EPFL, Lausanne, Switzerland

*Equal contribution

[#]Correspondance: Franziska Bleichert
franziska.bleichert@yale.edu

Table of Contents:

Appendix Figure S1 …………………………………………………………………… Page 2
Appendix Figure S2 …………………………………………………………………… Page 4
Appendix Figure S3 …………………………………………………………………… Page 5
Appendix Figure S4 …………………………………………………………………… Page 6
Appendix Figure S5 …………………………………………………………………… Page 7
Appendix Figure S6 …………………………………………………………………… Page 8
Appendix Figure S7 ………………………………………………………………….... Page 9
Appendix References ………………………………………………………………….. Page 10

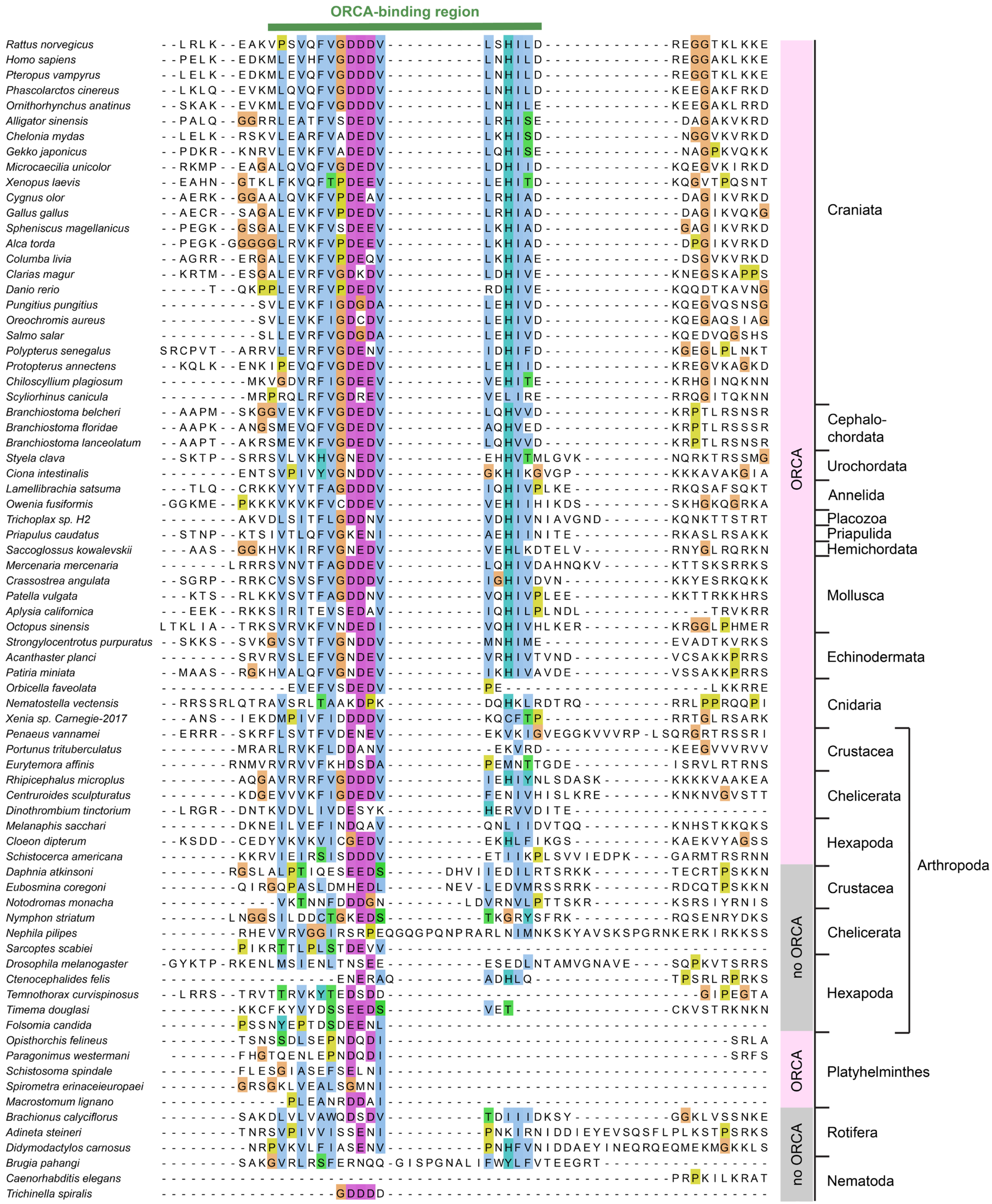

Appendix Figure S1. Conservation of the ORCA-binding sequence in Orc2 across the metazoan kingdom. The presence of ORCA in different phyla and/or subphyla is indicated. Note that some orders in the phylum Arthropoda appear to encode an ORCA ortholog (as defined by a conserved

WD40 domain) while others do not, and that ORCA orthologs in the phylum Platyhelminthes are very long polypeptides and may utilize alternative mechanisms to associate with Orc2 (see also **Table 2**).

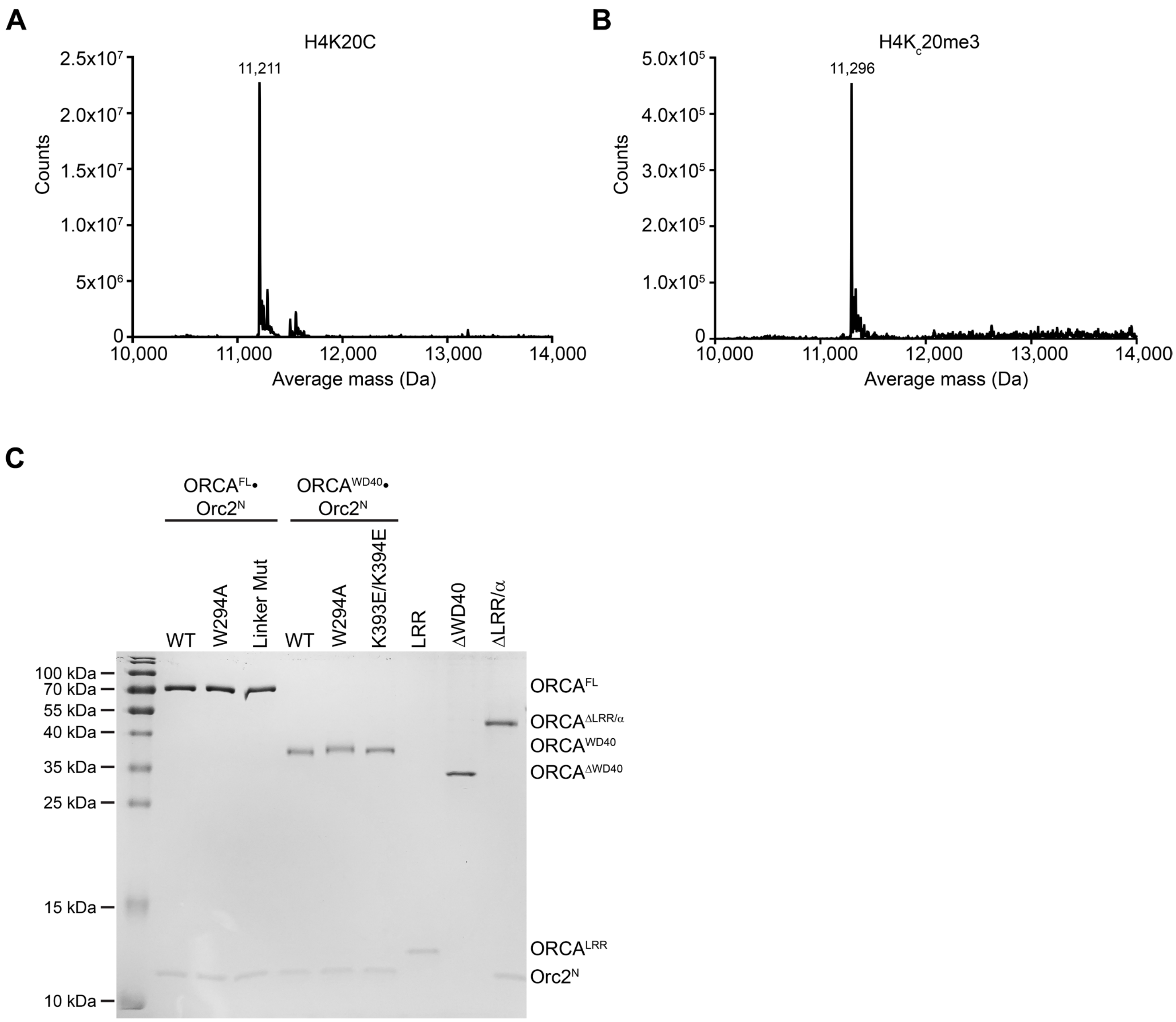

Appendix Figure S2. Mass spectrometry of histone H4 containing the trimethyl-lysine analog (MLA) and SDS-PAGE of purified ORCA constructs.

A-B. Intact mass spectrometry of H4 before and after MLA installation. The mass difference between H4K20C (in A) and H4K$_c$20me3 (in B) indicates successful MLA installation.

C. Coomassie-stained SDS-PAGE gel of purified *Rn*ORCA proteins used in this study.

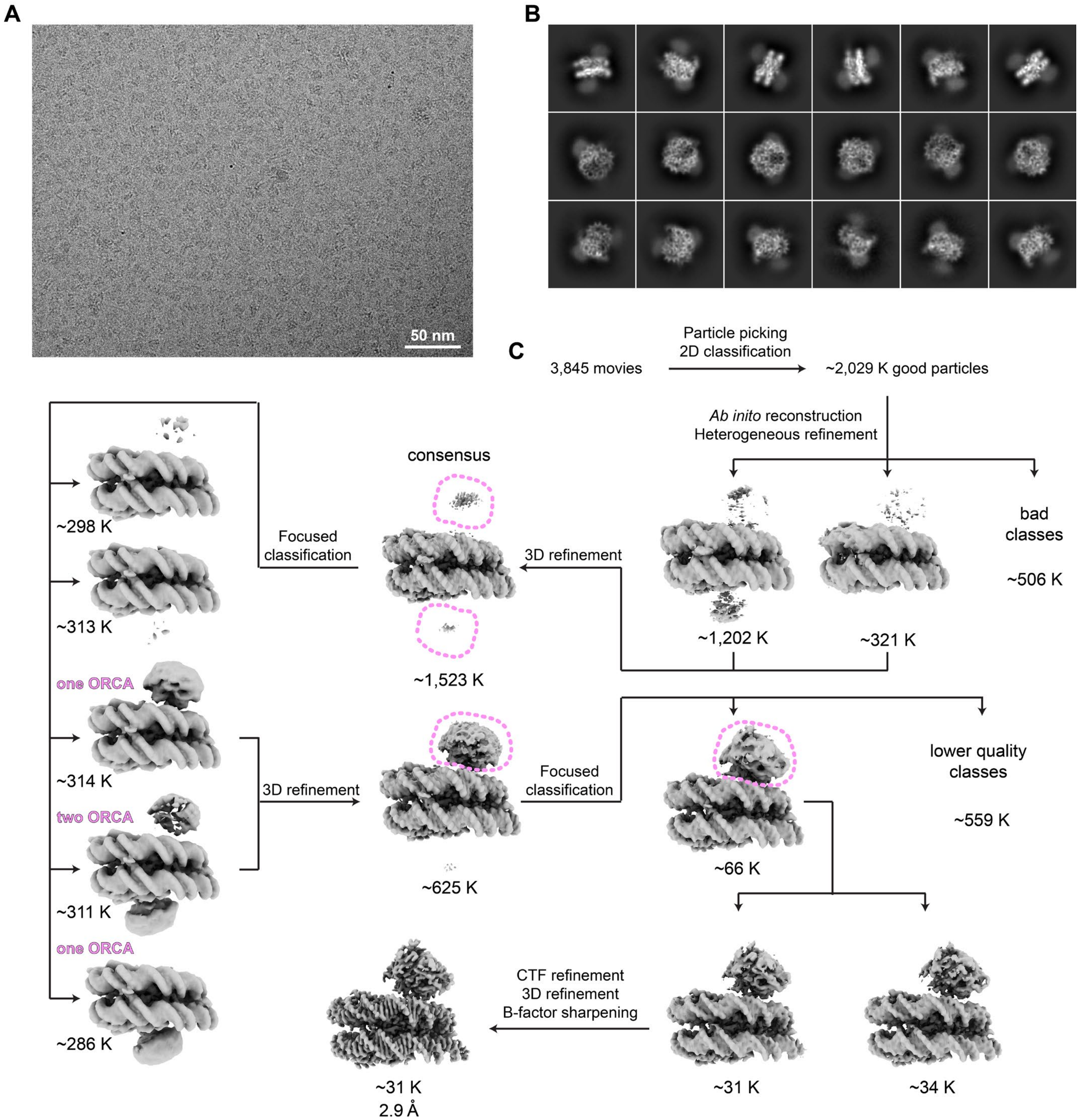

Appendix Figure S3. Summary of cryo-EM data processing workflow.

A. Representative image of summed movie frames.

B. 2D class averages of the ORCA^{FL}•Orc2^{N}•H4K20me3-nucleosome complex.

C. Data processing scheme used to obtain the 2.9 Å map of the ORCA^{FL}•Orc2^{N}•H4K20me3 nucleosome complex. Dotted lines indicate masks used for focused 3D classification. Note that one of the two ORCA WD40 domains bound to a nucleosome is averaged out during 3D reconstruction due to substoichiometric occupancy and/or flexibility (see also **Appendix Fig S4D**).

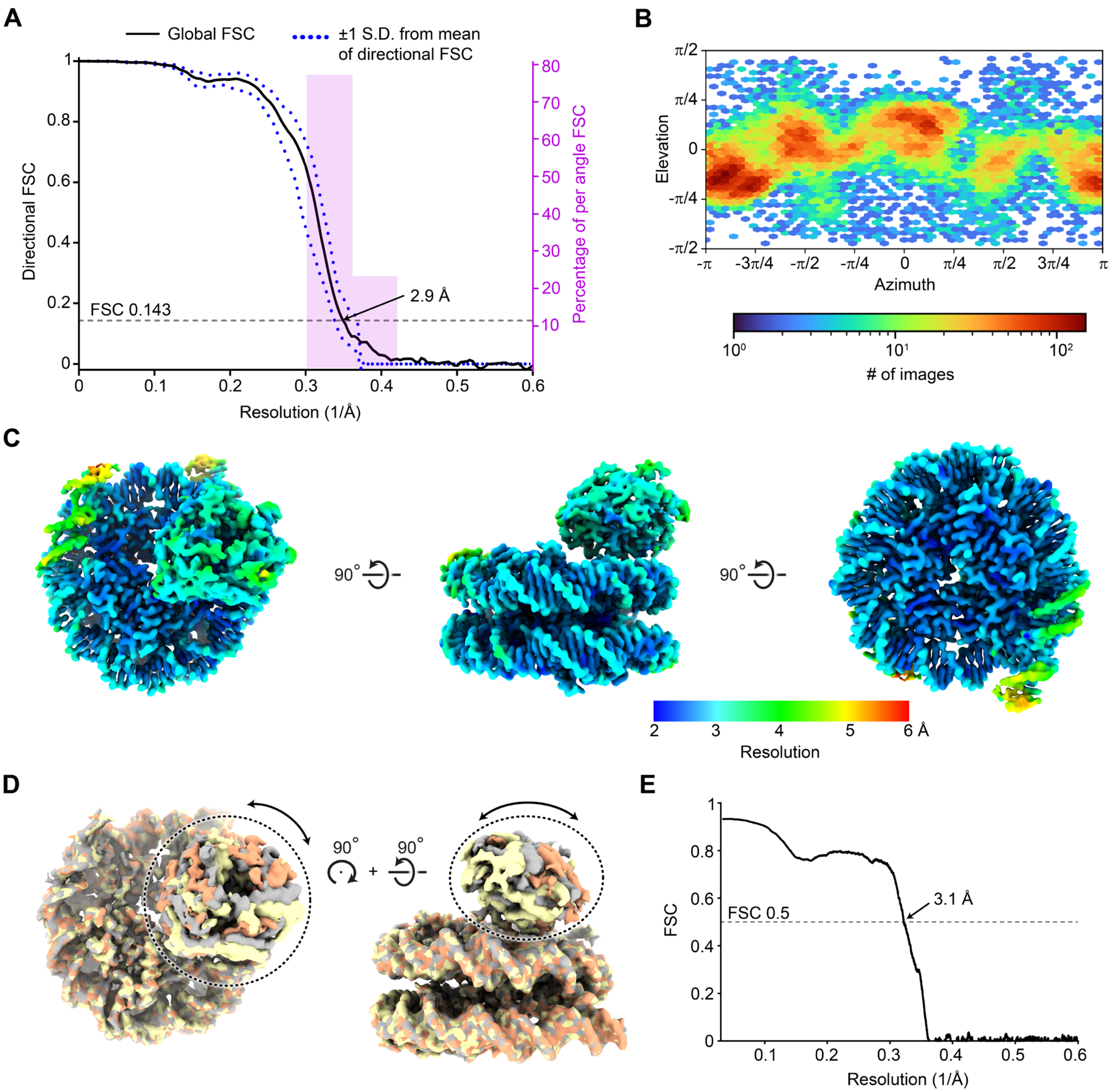

Appendix Figure S4. Resolution and angular particle distributions for the ORCA^{FL}•Orc2^{N}•H4K20me3-nucleosome cryo-EM structure.

A. ThreeD Fourier shell correlation (FSC) analysis (Tan et al, 2017) of the reconstructed cryo-EM map.

B. Angular distribution of particles contributing to the final reconstruction.

C. Sharpened cryo-EM map of the ORCA^{FL}•Orc2^{N}•H4K20me3-nucleosome complex colored by local resolution.

D. Superposition of three different 3D class volumes (low-pass filtered to 4 Å) illustrates flexibility of ORCA bound to a nucleosome, limiting the local resolution of ORCA. Despite the flexibility, similar ORCA•nucleosome contacts are formed.

E. FSC curve calculated using the final refined model and cryo-EM map.

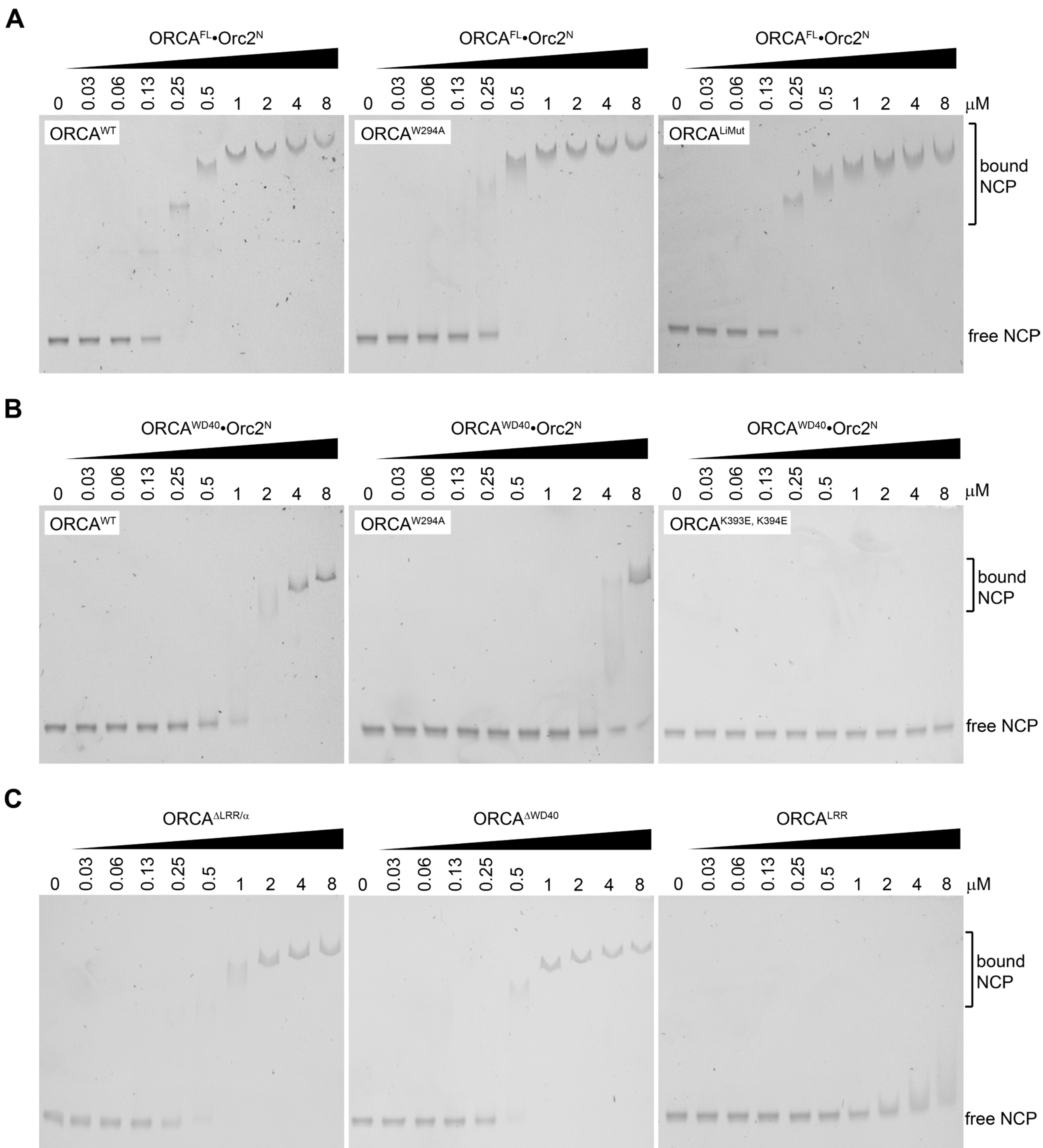

Appendix Figure S5. Examples of EMSA gels for H4K20me3-mononucleosome binding by ORCA. See **Figs 2H, 3B, and 5B** for binding curves.

A. EMSA gels for wildtype or mutant full-length ORCA binding to H4K20me3-mononucleosomes.

B. EMSA gels for wildtype or mutant ORCA-WD40 domain binding to H4K20me3-mononucleosomes.

C. EMSA gels for binding of other truncated ORCA constructs to H4K20me3-mononucleosomes.

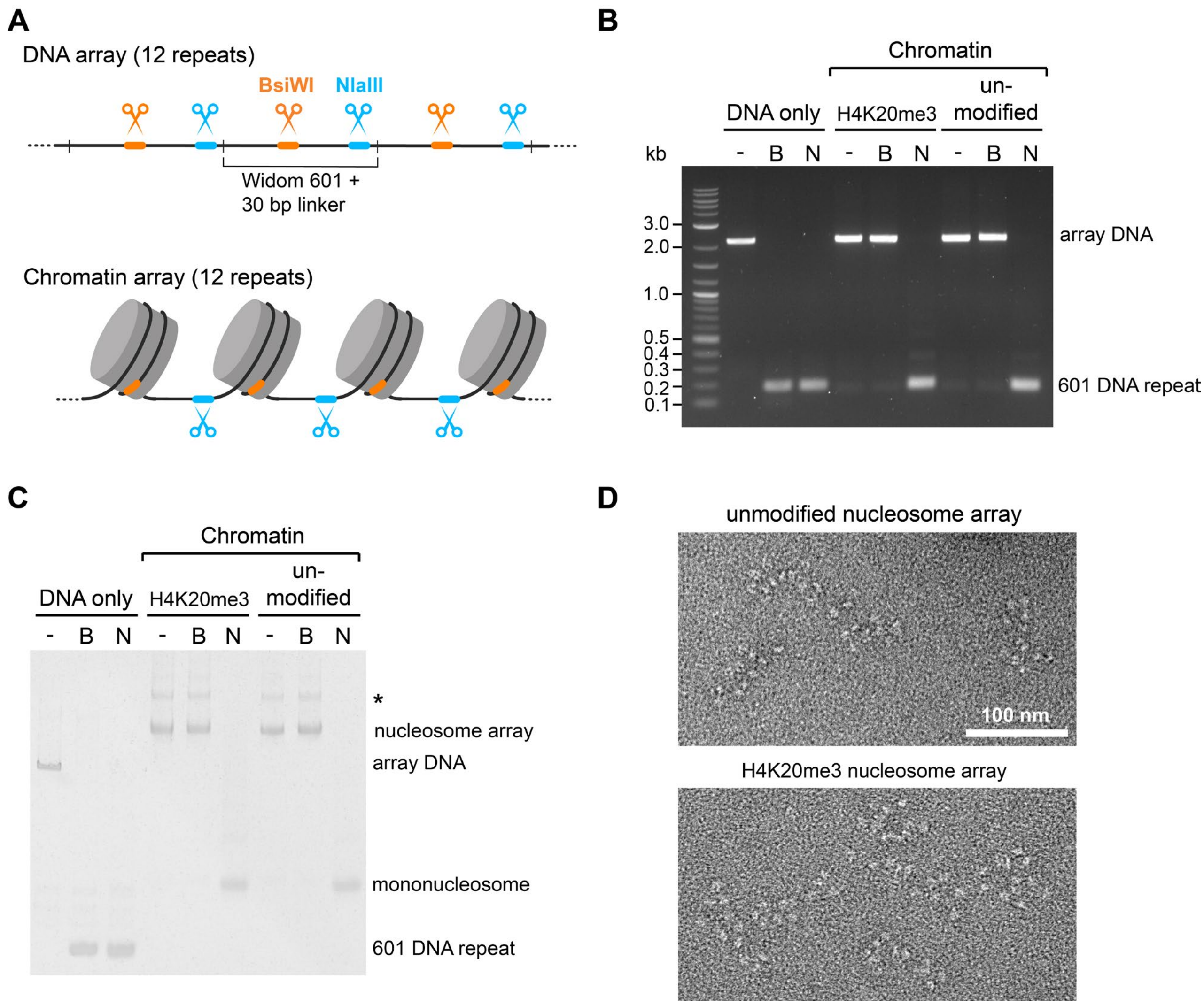

Appendix Figure S6. Reconstitution of nucleosome arrays.

A. DNA arrays comprising 12 repeats of the Widom 601 nucleosome positioning sequence separated by 30 bp linkers were used to reconstitute chromatin arrays. Successful reconstitution was validated by restriction digest with BsiWI and NlaIII. BsiWI only cleaves free DNA since the recognition site in the Widom 601 sequence is protected upon nucleosome formation. The NlaIII recognition site is located in the linker region and is cleaved both in free DNA and nucleosome arrays.

B. Agarose gel electrophoresis of free array DNA and reconstituted H4K20me3- and unmodified chromatin arrays after BsiWI (B), NlaIII (N), and mock (-) restriction digestion followed by proteinase K treatment.

C. Native agarose-polyacrylamide gel electrophoresis of free array DNA and reconstituted H4K20me3- and unmodified chromatin arrays after BsiWI (B), NlaIII (N), and mock (-) restriction digestion (without proteinase K treatment). Asterisk denotes a chromatin oligomer observed in some reconstitutions.

D. Electron micrograph of negatively stained unmodified and H4K20me3-modified nucleosome arrays.

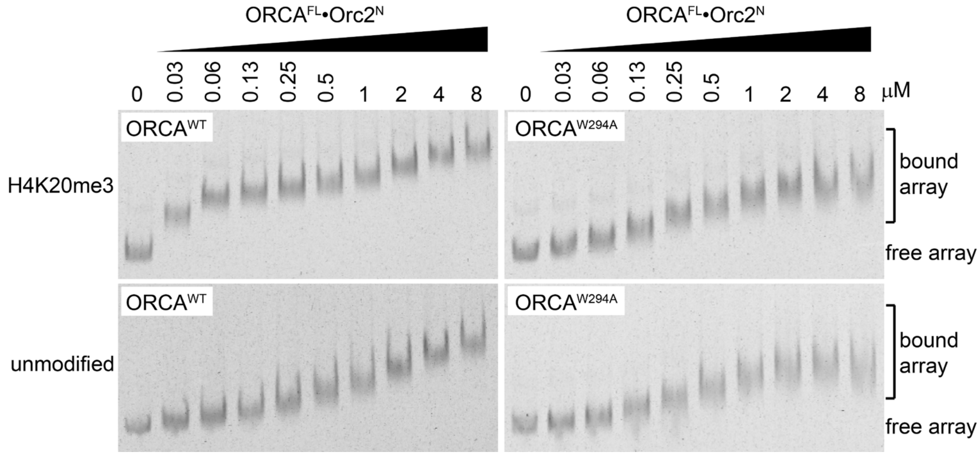

Appendix Figure S7. The aromatic cage in ORCA's WD40 domain is required for high-affinity chromatin binding. Native agarose-polyacrylamide gels of EMSA assays comparing binding of full-length, wildtype ORCA and that harboring the W294A mutation in the aromatic cage to nucleosome arrays. The aromatic cage mutation abolishes ORCA's ability to distinguish H4K20me3- and unmodified arrays. The gels for ORCA^{WT} are reproduced from **Fig 3D** for direct comparison.

Appendix References

Tan YZ, Baldwin PR, Davis JH, Williamson JR, Potter CS, Carragher B, Lyumkis D (2017) Addressing preferred specimen orientation in single-particle cryo-EM through tilting. *Nat Methods* **14:** 793-796